

Random three-dimensional jammed packings of elastic shells acting as force sensors

(Dated: May 27, 2016)

I. SUPPORTING INFORMATION

A. Force law

When two spherical shells of radius R are in contact with a contact force F they each deform from a spherical shape. For small forces the deformation is a slight flattening localized around the point of contact. The deflection of the contact point is $\delta/2$ in our notation, and is given by [1]:

$$F_L = k \frac{\delta}{R}, \quad (1)$$

where $k = 2Ed^2/\sqrt{3(1-\nu^2)}$ and ν the Poisson ratio. If the contact force in a low volume fraction packing is calculated using Eq. 1 for all δ values we obtain the force distribution shown in Fig. S1B (black points). However, more than 50% of contacts deform by a large force, as shown by Fig. S1A. For larger forces one of the shells buckles, resulting in a dimple with inverted curvature. The relation between force and deflection is now given by Ref 2, 3

$$F_{NL} = c\sqrt{\frac{\delta}{R}}, \quad (2)$$

where $c = 0.534Ed^{5/2}\pi/(1-\nu^2)\sqrt{R}$. Fig. S1C compares these two analytical results, which intersect at $\delta_c/R = (c/k)^2$. The force distribution calculated with Eq. 2 is shown in Fig. S1B (blue points), but it seriously underestimates the number of small forces in the packing. If the force distributions are calculated from the experimental data using Eq. 1 for $\delta_{i,j} < \delta_c$ and Eq. 2 for $\delta_{i,j} > \delta_c$ we obtain distributions with unphysical discontinuities, as shown in Fig. S1B (red points). The low value is caused by the narrower width of the last bin used for binning data with Equation 1. An analytical formula interpolating smoothly between these limits is not known, although many numerical results exist, *e.g.* Ref. 4.

A suitable formula that accomplishes this can be found by starting with the assumption that the total deflection is the sum of that due to the linear contribution, which is localized near the apex, and the nonlinear contribution, which is due to the dimple formation [5, 6]. Thus, writing $x = \delta/R$ we find:

$$x = F/k + F^2/c^2. \quad (3)$$

Solving for F leads to

$$F_{COMB} = \frac{c^2}{2k} \left(\sqrt{1 + \frac{4k^2}{c^2}x} - 1 \right). \quad (4)$$

This curve is compared with Eqs. 1 and 2 in Fig. S1C (green curve). While it correctly describes the limits for small and large x the convergence at large x is unsatisfyingly slow due to the term -1 in Eq. 4. To improve this we add an empirical term that corresponds to a sigmoidal curve that climbs from 0 to $c^2/2k$ around the crossover point $x_c = (c/k)^2$:

$$F_{STITCHING} = \frac{c^2}{2k} \left(\sqrt{1 + \frac{4k^2}{c^2}x} - 1 + 0.92 \frac{x^2}{x^2 + (c/k)^4} \right). \quad (5)$$

The added term has no linear term in its Taylor expansion to avoid interference with the low x limit. Furthermore, we give it a prefactor slightly below 1 to produce an optimal fit in the relevant range $0 < x < 1$. It is compared with the other curves in Fig. S1C (red curve). Differences with Equations 1 and 2 are very small.

To validate our stitching force law against experimental data we compare it to Atomic Force Microscopy measurements from Ref. 7 on similar shells of radius 365 nm and three different shell thicknesses. It is seen that Eq. 5 describes the data quite well, providing confidence in its validity. The force distribution obtained using this force law is shown in Fig. S1B (green points). A smooth distribution is found that matches the ones found using only small or only large forces in their respective ranges.

B. Force network

A quantitative analysis of force chains was performed based on a definition for a force chain that avoids the branching and merging of the force network, as described in the article by Desmond *et al.* [8]. From their definition a force segment belongs to a force chain if it is one of the two largest forces on both particles joined by the force segment. In this way the maximum number of forces on a particle is limited to two, thereby avoiding branching of the chains. In addition to this we set the limit of the minimum length of a force chain to three particles, or two force segments. Note that in this definition even small forces below average can also become a part of force chain, provided it is the largest for the given particle and its contacting neighbor. The average length of the chains in our jammed shell packings at various φ and at various shear amplitudes are given in the Table S2.

For further investigation of the correlation in the direction of the force segments within chains, we plotted the probability of the angle (α) between the force segments in a force chain normalized by the unit solid angle, as shown in Fig. S3 A and B for compression and shear. The probability $P(\alpha)/\sin(\alpha)$ is non-uniform in both cases: it has a small peak at α around 60° and a high peak near 180° .

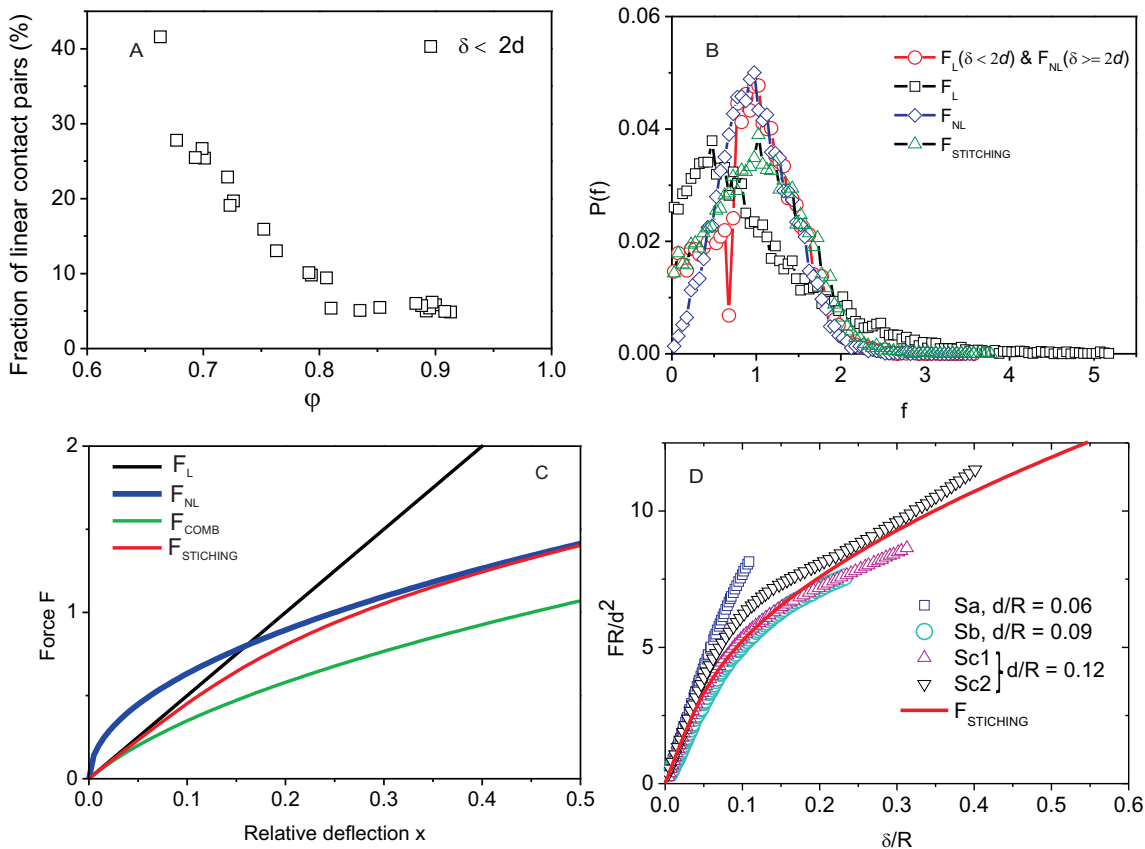


FIG. S1. (A) Plot of the fraction of contacts at volume fraction 0.663 for which the deformation depth (δ) is less than twice the shell thickness (d), expected to obey a linear force-distance law. (B) A typical distribution of contact forces in a low volume fraction packing of shells ($\phi = 0.663$) calculated using the linear force law (black), non-linear force law (blue), a force laws that is linear for $\delta < 2d$ and nonlinear for $\delta \geq 2d$ (red), and the stitching force law (green). (C) Force-deflection graph showing the linear (black) and square root (blue) laws, their combination Eq. 4 (green), and the stitching law Eq. 5. Curves were drawn for $k = 5$ and $c = 1$. (D) A test of the validity of Eq. 5 using experimental data from Ref. 7.

For all volume fractions and shear strains the probability is strongly suppressed for $\alpha < 60^\circ$ due to the narrow size distribution of the shells. The peak around 60° indicates an enhanced tendency for larger forces to form trimers in the system; a similar peak was also observed in experiments on monodisperse compressed emulsions [9]. However, the peak height is rapidly reduced and is shifted to higher angles with increasing volume fraction ϕ . In addition, for the packing, $\phi = 0.810$ (Fig. S3 A), we find more or less three prominent peaks: around 60° , 120° and near 180° , which again is a sign that there is local ordering in the sample, but not confirmed by local bond order analysis [10]. For shear deformation, the probability at 180° is found to be slightly higher compared to that in compression, but there is no big change with increase in shear strain (Table S2).

From the distribution $P(\alpha)/\sin(\alpha)$ we measured the persistence length of the chains given by [11],

$$\ell^* = \langle 2R_t \rangle / (1 - \langle \cos(180 - \alpha) \rangle) \quad (6)$$

where $\langle 2R_t \rangle$ is the mean diameter of the particle. Table S2 shows the persistence length of force chains at different volume fractions and for different strain amplitudes plotted in Fig. S3 A and B. The value of the persistence length is smaller than the average length of the chain, especially for compression. However, clearly long-range chain like correlation is higher in the shear experiments as compared to a uniaxial compression.

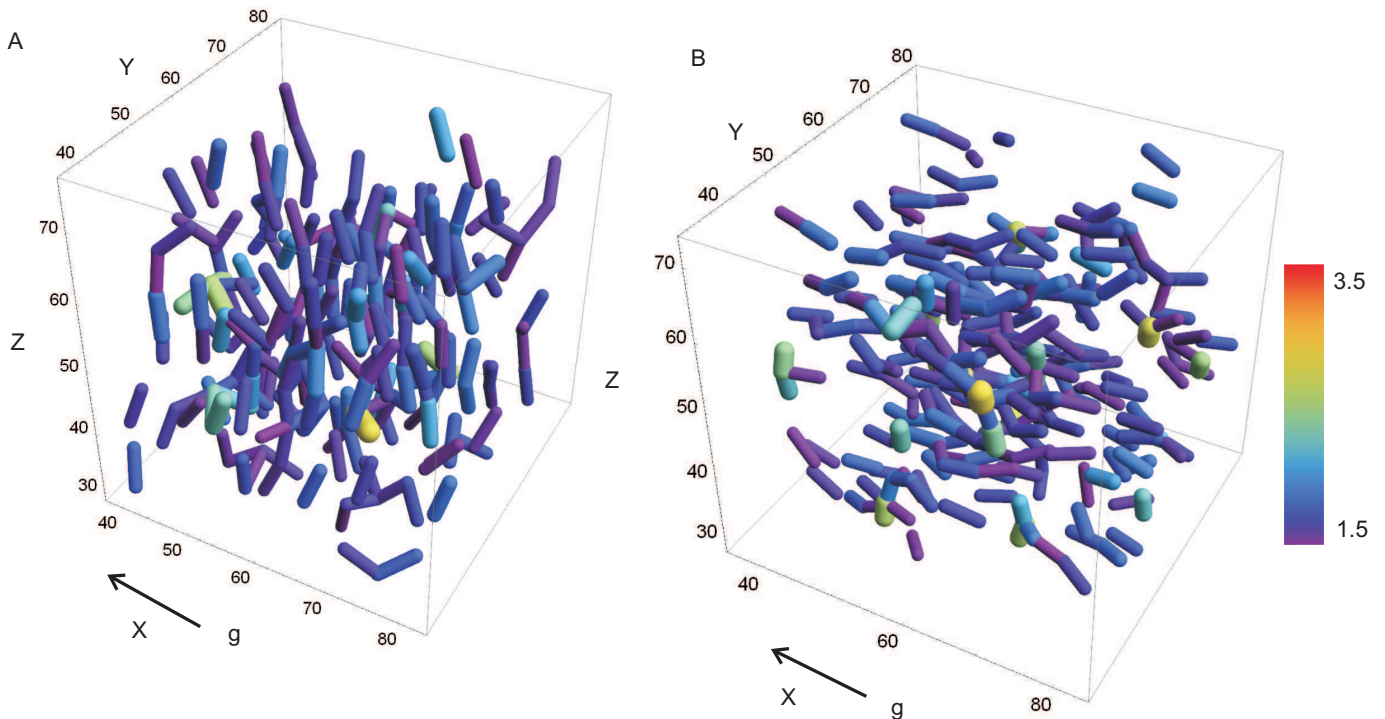


FIG. S2. A magnified view of Fig. 5, the force networks in compressed shells in the lowest and highest packing fractions, (A) $\varphi = 0.699$ and (B) $\varphi = 0.908$ for forces greater than 1.5 times the average value. Forces, in units of the average force $\langle F \rangle$ are represented by tubes connecting the centers of contact pairs where the thickness and color of the tube is proportional to the magnitude of the normal force. Red indicates a force 3.5 times larger than the average force. The X -axis is the direction of gravity.

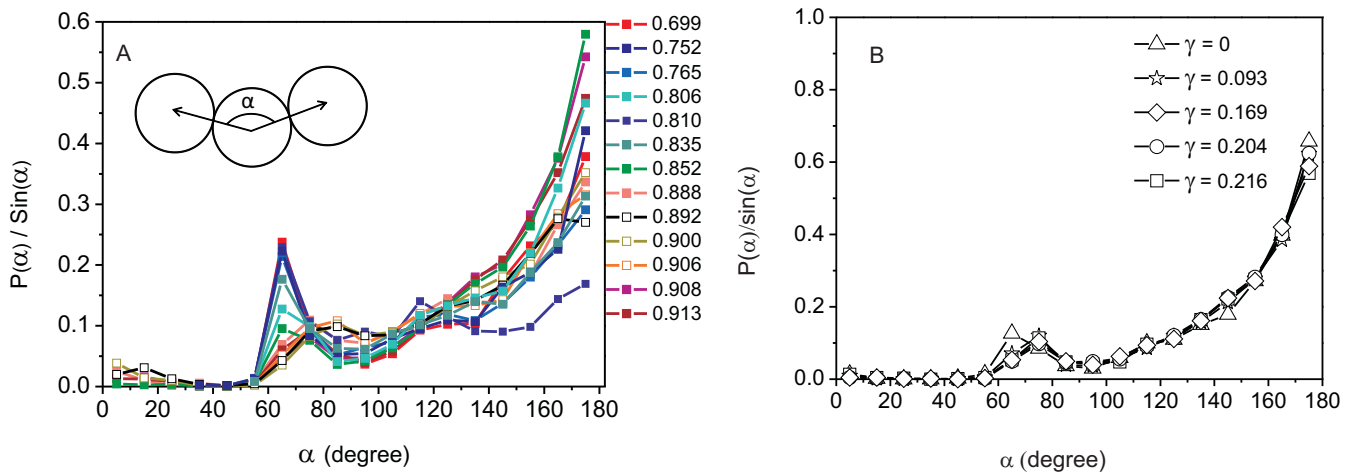


FIG. S3. Distribution of angle between the force segments in force chains normalized by the solid angle in packings at various (A) φ and (B) shear strain amplitudes. The main effect of the shear was to displace the small local maximum from 60° to about 75° or a deformation of the local order around a particle.

TABLE S1. The value of average contact force and pressure measured at different volume fractions in the static shell packings containing shells of $d/R_t = 0.02$, except for image stack T1 which corresponds to shells of $d/R_t = 0.04$.

Image stack	φ	$\langle F \rangle$ (μN)	Pressure (KPa)
S1	0.892	0.079	18.92
S2	0.913	0.077	18.22
S3	0.900	0.076	17.12
S4	0.895	0.075	16.45
S5	0.908	0.074	16.67
T1	0.906	0.275	29.21
S6	0.897	0.074	15.92
S7	0.888	0.072	15.36
S8	0.883	0.068	13.99
S9	0.852	0.067	12.68
S10	0.835	0.063	11.31
S11	0.806	0.058	9.61
S12	0.810	0.059	10.27
S13	0.793	0.057	9.25
S14	0.791	0.054	8.69
S15	0.765	0.054	8.10
S16	0.763	0.058	7.62
S17	0.776	0.053	8.11
S18	0.752	0.049	6.93
S19	0.726	0.046	5.88
S20	0.721	0.044	5.34
S21	0.723	0.046	5.89
S22	0.701	0.042	4.67
S23	0.699	0.042	4.63
S24	0.693	0.043	4.65
S25	0.677	0.041	3.98
S26	0.663	0.031	2.56

TABLE S2. Average lengths and persistence lengths of force chains obtained from jammed shell packings at different volume fractions and for different strain amplitudes.

φ	average chain length $\times \langle 2R_t \rangle$	Persistence length (ℓ^*) $\times \langle 2R_t \rangle$
0.699	4.45	2.31
0.752	4.35	2.26
0.765	5.25	2.08
0.806	5.68	2.85
0.810	5.33	1.61
0.835	4.30	2.22
0.852	5.89	3.43
0.885	4.86	2.27
0.888	4.65	2.32
0.900	6.10	2.43
0.906	4.96	2.62
0.908	5.23	3.49
0.913	6.21	3.11
Measured strain		
0	4.42	3.31
0.093	4.61	3.51
0.169	4.66	3.64
0.204	4.93	3.76
0.216	4.63	3.46

-
- [1] Reissner, E., *J. Math. Phys.* **25**, 279 (1946).
- [2] L. D. Landau and E. M. Lifshitz, *Theory of Elasticity* (Pergamon, New York, 1986).
- [3] A. V. Pogorelov, *Bendings of surfaces and stability of shells* (American Mathematical Society, Providence, 1988).
- [4] A. Nasto, A. Ajdari, A. Lazarus, A. Vaziri, and P. M. Reis, *Soft Matter* **9**, 6796 (2013).
- [5] A. Y. Evkin, *Int. J. Solids Struct.* **42**, 1173 (2005).
- [6] G. V. Ranjan, In: *Proceedings. AIAA J/ASME 18th Structural Dynamics and Materials Conference*. San Diego, California, 269 (1977).
- [7] C. I. Zoldesi, I. L. Ivanovska, C. Quilliet, G. J. L. Wuite, and A. Imhof, *Phys. Rev. E* **78**, 051401 (2008).
- [8] K. W. Desmond, P. J. Young, D. D. Chen, and E. R. Weeks, *Soft Matter* **9**, 3424 (2013).
- [9] J. Zhou, S. Long, Q. Wang, and A. D. Dinsmore, *Science* **312**, 1631 (2006).
- [10] J. Jose, G. A. Blab, A. van Blaaderen, and A. Imhof, *Soft Matter* **11**, 1800 (2015).
- [11] J. Zhou and A. Dinsmore, *J. Stat. Mech.: Theory Exp.* **2009**, 05001 (2009).